

Radio spectral index from NVSS and TGSS

Prabhakar Tiwari^a and Adi Nusser^a

^aPhysics Department and the Asher Space Research Institute - Technion, Haifa 32000, Israel

E-mail: ptiwari@physics.technion.ac.il

Abstract. We extract the radio spectral index, α , from the 541,195 common sources observed in 150 MHz TIFR GMRT Sky Survey (TGSS) and 1.4 GHz NRAO VLA Sky Survey (NVSS). These catalogs cover about 80% of the sky and represent the largest radio population. We confirm the steepening of α with increasing flux density. Further, we observe an increase in α with source size (TGSS measured) saturating around size 50 arcsec to 0.83 ± 0.01 . From this saturated value, we constrain the electron energy injection spectral index, γ , and the fractional contribution of supernova remnants to the total radio flux. Our results indicate relatively low $\gamma \sim 1.8 - 1.9$ and a large supernova remnants contribution ($\sim 15 - 25\%$). For very compact sources the convection and the thermal radio emission are likely to be important.

Keywords: supernova remnants - radio continuum, cosmic rays - ISM, galaxies: high-redshift, galaxies: active

Contents

1	Introduction	1
2	Data	2
2.1	TGSS	2
2.2	NVSS	2
2.3	TGSS-NVSS cross matching	3
3	Theory	3
3.1	Thermal radio emission	3
3.2	Non-thermal radio emission	3
3.2.1	Radio emission from SNRs	3
3.2.2	Radio emission from cosmic ray diffusion	4
3.2.3	Radio emission from cosmic ray convection	4
4	Observed spectral index	4
5	Results and analysis	5
5.1	Radio spectral index dependence on flux density	5
5.2	Radio spectral index dependence on size	5
5.3	Escape probability P_{esc}	5
6	Summary and Discussion	6
7	Acknowledgments	7

1 Introduction

The radio emission from a distant galaxy consists of thermal and synchrotron emission. The thermal emission is bremsstrahlung from H II regions and the synchrotron emission is expected to arise from supernova remnants (SNRs) and diffuse cosmic ray electrons (CREs) spread over the disk and halo [1, 2]. Interestingly, the radio emission from all these components follows a different spectral index and the total spectral index depends on their relative contribution. The thermal radio emission is almost flat ($\propto \nu^{-\alpha}$) with spectral index $\alpha = 0.1$ [2], whereas, the synchrotron emission from SNRs is steep with spectral index $\alpha = 0.5$ [2–5] and the synchrotron emission from diffuse CREs is even more steeper with spectral index α ranging from 0.5 to 1.1 [2, 3, 6]. The diffuse CREs spectral index depends on the physical mechanism of CREs propagation i.e. the CREs can diffuse through the galaxy by random scattering in the irregular magnetic field or by convection. In the diffusion and convection processes, the CREs can escape from the galaxy, the probability of escaping decrease with increasing size of the radio source.

Ideally one needs to spatially resolve a radio source to disentangle above radio emission components, however, from the total spectral index, several conclusions about the relative contribution from SNRs and the CREs propagation processes i.e. diffuse/convection can be achieved [6]. In the present paper, we prepare a unique source catalog from TIFR GMRT Sky Survey (TGSS) [7] and NRAO VLA Sky Survey (NVSS) [8], and employ this to explore radio galaxy emission processes. We find total 541,195 unique sources common in both TGSS and NVSS, and study the dependence of spectral index on flux and source size. The size dependence study enables us to draw statistical conclusions about emission components and diffusion processes. Assuming that the source population peaks between redshift $z \approx 0.5 - 1$ [9, 10], our results roughly corresponds to radio population at $z = 0.5 - 1$, the survey flux limits are such as the most of the sources are presumably AGNs.

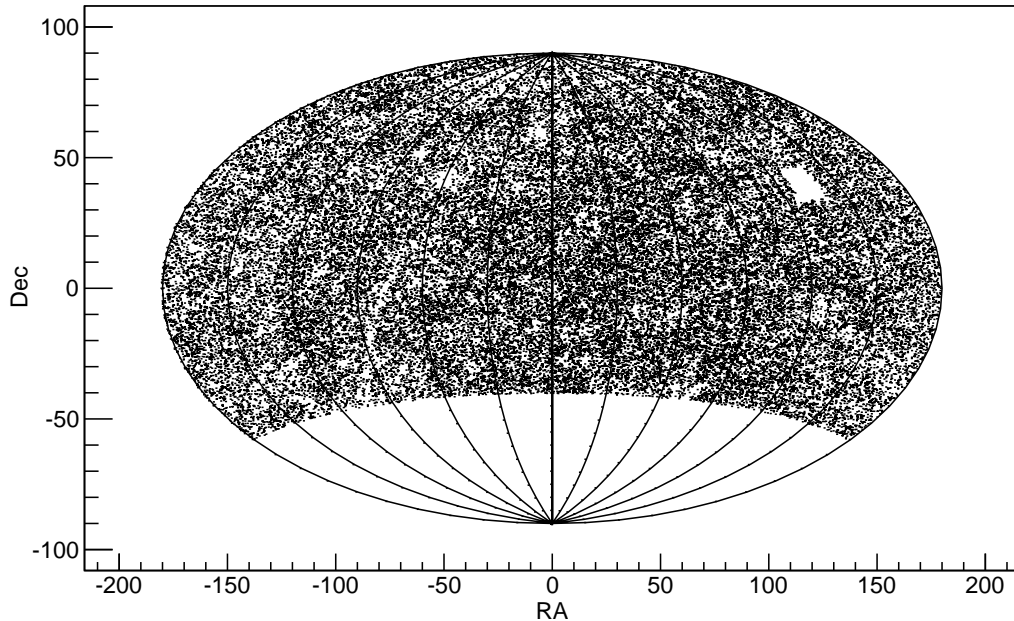


Figure 1: The spatial distribution of NVSS-TGSS common sources. Note that only 10% sources are shown as if we project all 541,195 sources, the figure becomes very dark.

The outline of the paper is as following. We discuss the NVSS and TGSS data and describe the cross matching procedure in Section 2. In Section 3 we discuss the basic mechanisms of radio emission and their spectral index. We describe the observed spectral index in terms of different radio emission processes and escape probability in Section 4. In Section 5 we give all our results and analysis. We conclude with discussion in Section 6.

2 Data

2.1 TGSS

The TGSS catalog is from the Giant Metrewave Radio Telescope (GMRT), located 80 km north of Pune, India; performing all-sky radio continuum survey at 150 MHz [11]. The catalog is surveyed between 2010 and 2012 and recently been published by Intema et al. (2016)[7]. The catalog almost covers 90% of the full sky at 150 MHz with median RMS brightness fluctuations 3.5 mJy/beam at resolution $25'' \times 25''$ north of 19° DEC and $25'' \times 25'' / \cos(\text{DEC} - 19^\circ)$ south of 19° . The catalog contains total 623,604 sources (489,570 sources above flux 50 mJy) observed at seven sigma peak-to-noise threshold. The catalog RA, DEC (source centroid position) accuracy is better than $2''$ [7].

2.2 NVSS

The NVSS catalog contains ~ 1.7 million sources at 1.4GHz with flux $S_{1.4\text{GHz}} > 2.5$ mJy [8]. This flux limit at 1.4GHz very well covers the TGSS flux limits (at 150 MHz). The full width at half maximum angular resolution is $45''$ and nearly all observation is performed at uniform sensitivity. The catalog covers almost 82% of the sky and has its 100% overlap with TGSS. The RMS uncertainty in RA and DEC is up to $7''$.

2.3 TGSS-NVSS cross matching

For each 623,604 TGSS sources, given the TGSS angular position, we identify the NVSS sources with the distance less than $30''$. In total we find 553,301 TGSS sources having at least one NVSS source within $30''$. A few of TGSS sources have more than one NVSS association with our search criteria of $30''$, we drop these to avoid confusion and artificial scatter in the spectral index. At last, we identify total 541,195 unique sources. Each of this source is uniquely identified in both TGSS and NVSS and has one to one correspondence. The spatial distribution of these common sources is shown in Fig.1.

3 Theory

3.1 Thermal radio emission

The thermal radio emission is produced by deflection of electrons (bremsstrahlung) in H II regions. The H II regions are presumed to be photoionized by stars and the thermal emission from these regions is proportional to the production rate, N_{uv} , of Lyman continuum photons. An estimate for N_{uv} can be followed from [2],

$$\left(\frac{N_{\text{uv}}}{s^{-1}}\right) \gtrsim 6.3 \times 10^{52} \left(\frac{T_e}{10^4\text{K}}\right)^{-0.45} \left(\frac{\nu}{\text{GHz}}\right)^{0.1} \left(\frac{L_T}{10^{20}\text{WHz}^{-1}}\right). \quad (3.1)$$

Here L_T is the thermal luminosity and T_e is the electron temperature. The thermal luminosity L_T can be expressed in terms of thermal radio flux density S_T as $L_T = 4\pi d^2 S_T$, following equation (3.1) this indicate,

$$S_T \propto \nu^{-0.1}, \quad (3.2)$$

at high frequencies (\sim GHz) when the electron deflection opacity is small, the approximate thermal radio emission S_T with respect to non-thermal radio emission S_{NT} is given as [12],

$$\left\langle \frac{S_{\text{NT}}}{S_T} \right\rangle \sim 10 \left(\frac{\nu}{\text{GHz}}\right)^{0.1-\alpha}, \quad (3.3)$$

where $\alpha \sim 0.8$ is approximate non-thermal spectral index. This suggests that the thermal contribution in total flux at 1.4 GHz is $\sim 10\%$ and at 150 MHz it is $\sim 3\%$ i.e. the dominant part is non-thermal emission.

3.2 Non-thermal radio emission

The non-thermal radio emission contains two parts: the synchrotron emission from SNRs and the diffuse synchrotron emission from cosmic rays scattered by diffusion/convection in the galactic disk and halo.

3.2.1 Radio emission from SNRs

The synchrotron emission from SNRs is estimated assuming the simple leaky box model [6]. The cosmic electrons produced from supernovae can be described as a power law,

$$Q(E) = f_{\text{SN}} n_{\text{SN}} \left(\frac{E}{E_0}\right)^{-\gamma}. \quad (3.4)$$

Here $Q(E)$ is the production rate of the CREs from a supernova, f_{SN} the supernova production rate, n_{SN} the number of CREs produced per energy interval per supernova, and γ the energy injection spectral index. Let τ be the lifetime of the supernova remnant, then the number of electrons with energy E in energy bin dE can be given as,

$$\frac{\partial N(E)}{\partial t} + \frac{N(E)}{\tau} = Q(E). \quad (3.5)$$

For steady state ($\frac{\partial N(E)}{\partial t} = 0$) the solution to equation (3.5) is,

$$N(E) = Q(E)\tau. \quad (3.6)$$

With assumption that all electrons in magnetic field strength B , with energy E emit synchrotron radiation at frequency ν [6, 13],

$$\nu = 4.65 \left(\frac{E}{1\text{GeV}} \right)^2 \left(\frac{B}{\mu\text{G}} \right) \text{MHz}. \quad (3.7)$$

We can write the total synchrotron emission $P(\nu)$ at frequency ν in frequency interval $d\nu$ as,

$$P(\nu)d\nu = N(E) \left(\frac{dE}{dt} \right)_{\text{syn}} \left(\frac{dE}{d\nu} \right) d\nu. \quad (3.8)$$

The energy loss by synchrotron radiation $\left(\frac{dE}{dt} \right)_{\text{syn}} \propto B^2 E^2$ [6], and following from equation (3.4), (3.6), (3.7) and (3.8), we obtain $P(\nu) \propto \nu^{\frac{1-\gamma}{2}}$, i.e. $\alpha_{\text{SNR}} = (\gamma - 1)/2$. For $\gamma \approx 2$ [3, 14, 15] the power is approximately $\propto \nu^{-0.5}$.

3.2.2 Radio emission from cosmic ray diffusion

The CREs in galaxy propagate randomly due to magnetic field randomness, and also due to scattering, electrons effectively move outwards i.e. convection. The electrons moving in magnetic field lose energy by synchrotron radiation and inverse Compton scattering. Here we briefly discuss the diffusion model. The electron number density $N(E, r)$, at a distance r from source, in a simple diffusion model follows as,

$$\frac{\partial N(E, r)}{\partial t} - D(E)\nabla^2 N(E, r) - \frac{\partial}{\partial E}(b(E)N(E, r)) = Q(E, r), \quad (3.9)$$

where $D(E) \propto E^\mu$ is the diffusion coefficient and $b(E)$ is the energy losses due to inverse Compton and synchrotron emission. In the case of steady state ($\frac{\partial N(E, r)}{\partial t} = 0$), the solution to diffusion equation (3.9) is [6, 16],

$$N(E, r) \propto E^{-\gamma} E^{-\mu} \times (\text{confluent hypergeometric function}). \quad (3.10)$$

Following the formulation from section 3.2, equation (3.10) suggests the diffusion spectral index, $\alpha_{\text{diff}} = (\gamma + \mu - 1)/2$.

3.2.3 Radio emission from cosmic ray convection

The CREs may escape from their source by convection. The production rate $Q(E, r)$, following convection process is written as,

$$\nabla(vN(E, r)) - \frac{\partial}{\partial E}[\{(\nabla \cdot v)E + b(E)\}N(E, r)] = Q(E, r). \quad (3.11)$$

The approximate solution follows [6]¹, $N(E, z) \propto E^{-\gamma} \left(1 - \frac{bEz}{v}\right)^{\gamma-2}$, this indicates that approximately the convection spectral index, $\alpha_{\text{conv}} = (\gamma - 1)/2$.

4 Observed spectral index

We obtain the spectral index by comparing integrated radio emission from a source which is observed in both TGSS (150 MHz) and in NVSS (1.4GHz). The observed spectral index is the spatially integrated one and shaped by all possible radio emission processes. The radio thermal flux is almost

¹Lisenfeld & Völk (2000)[6] assume that the sources of CREs are situated in the galactic mid-plane ($z = 0$). $N(E, z)$ is the number of electrons at height z , with energy E in energy bin dE .

flat ($S \propto \nu^{-0.1}$), and for the TGSS and NVSS frequencies it is $\leq 10\%$ of the total flux. Therefore, the extracted spectral index,

$$\alpha_{\text{obs}} = (\log S_{\text{TGSS}} - \log S_{\text{NVSS}}) / (\log \nu_{\text{NVSS}} - \log \nu_{\text{TGSS}}), \quad (4.1)$$

can be approximated as a non-thermal spectral index. For each source, we compute α_{obs} using equation (4.1). If the fractional contribution from SNRs radio emission in total flux is f_{SNR} , and P_{esc} the escape probability of the diffusion electron then,

$$\alpha_{\text{obs}} = f_{\text{SNR}} \alpha_{\text{SNR}} + (1 - f_{\text{SNR}}) [\alpha_{\text{diff}} P_{\text{esc}} + \frac{\gamma}{2} (1 - P_{\text{esc}})]. \quad (4.2)$$

If the electron propagate by convection,

$$\alpha_{\text{obs}} = f_{\text{SNR}} \alpha_{\text{SNR}} + (1 - f_{\text{SNR}}) [\alpha_{\text{conv}} P_{\text{esc}} + \frac{\gamma}{2} (1 - P_{\text{esc}})]. \quad (4.3)$$

Note that for very extended sources when all the energy is lost due to synchrotron and inverse Compton losses, $P_{\text{esc}} = 0$, and $\alpha_{\text{diff/conv}} = \gamma/2$ [6]. This allows us to constrain the energy injection spectral index γ minus SNRs fraction f_{SNR} . For very large extended sources when observed spectral index α_{obs} becomes static with increasing size, $2\alpha_{\text{obs}} = (\gamma - f_{\text{SNR}})$.

5 Results and analysis

5.1 Radio spectral index dependence on flux density

We calculate the α_{obs} for each source following equation (4.1) and examine its dependence on flux density. Fig. 2 shows the α_{obs} distribution for sources with different TGSS (150 MHz) observed flux limits. Although the RMS spread is large, we see a clear trend of steepening of the spectral index with increasing flux. The large RMS spread is expected as an individual source may have very different radio emission processes and radio activity [9]. To explore this further, we plot the mean spectral index $\bar{\alpha}_{\text{obs}}$ with differential flux density bins in Fig.3. A liner fit $\bar{\alpha}_{\text{obs}} = (0.58 \pm 0.01) + (0.0799 \pm 0.005) \log_{10}(S_{\text{TGSS}}[\text{mJy}])$ very well represents the dependence. This confirms the earlier hints of spectral index dependence on flux density [17–21].

5.2 Radio spectral index dependence on size

As mentioned in section 4, the observed spectral index consists of radio emission from SNRs and diffusion/convection electrons. The diffusion/convection contribution depends on the source size as with increasing size the cosmic ray electron escape probability decreases (see equation (4.2) and (4.3)). In Fig. 4 we present the spectral index as a function of size (\sqrt{ab} in arcsec) measured in TGSS observation at 150 MHz. The observed spectral index rapidly increases with size for sources with size $\leq 26''$ and start saturating to a nearly size independent value beyond. The spectral index becomes independent of source size beyond $\sim 50''$, this is particularly interesting as the α_{obs} from these sources is presumably independent of cosmic ray propagation processes. For these ultra large sources the escape probability is zero, and α_{obs} is simply $(\gamma - f_{\text{SNR}})/2$. This enables us to constrain energy injection spectral index γ minus SNRs fraction f_{SNR} . We obtain this difference as 1.66 ± 0.02 . Assuming $\gamma = 2$ [3, 14, 15, 22], this suggests that the SNRs contribution in total radio flux is 34%. Alternatively, if we assume the SNRs contribution to be 10% [6], we find the energy injection spectral index $\gamma = 1.76 \pm 0.02$.

5.3 Escape probability P_{esc}

We calculate the escape probability (P_{esc}) for diffusion and convection processes for various sets of energy injection spectral index γ and SNRs contribution fraction f_{SNR} . We keep the difference $(\gamma - f_{\text{SNR}})/2$ equal to 0.83 to recover $P_{\text{esc}} = 0$ for ultra large size sources. We have shown our results in Fig. 5 and in Fig. 6. We have particularly shown the results for diffusion index $\mu = 0.6$ and with $\mu = 0.2$. The small value of μ represents the weak dependence of diffusion on energy. For

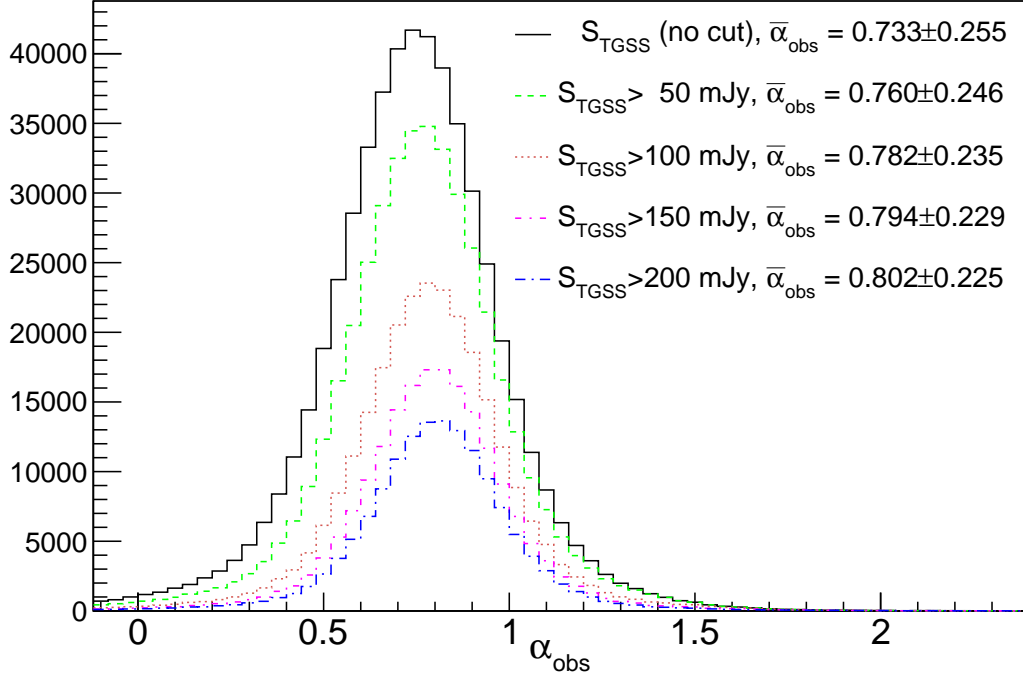


Figure 2: The NVSS-TGSS extracted radio spectral index with various TGSS flux density limits. We have 541,195 sources with no S_{TGSS} cut and 424,639; 266,885; 190,830; 147,171 sources with $S_{\text{TGSS}} > 50, 100, 150, 200$ mJy respectively. The ‘ \pm ’ error in $\bar{\alpha}_{\text{obs}}$ is RMS.

the energy relevant to radio emission ($> \text{GeV}$), $\mu = 0.4 - 0.7$ [23]. The very compact sources in Fig. 6 suggest a lower energy injection spectral index γ as to accommodate some contribution from diffusion/convection ($P_{\text{esc}} > 0$). Alternatively, maybe for the very compact sources, the thermal emission is also significant. Note that the thermal emission exhibits very flat spectral index ($\alpha = 0.1$).

6 Summary and Discussion

We have estimated the radio spectral index from NVSS and TGSS observed sources. We identify total 541,195 uniquely matched sources and study the size dependence of spectral index. The large number of sources enable us to study the spectral index in differential size bins. The spatially integrated spectral index, relevant to this work, consists of radio emission from SNRs and diffusion/convection electrons. We explore the source size dependence of observed spectral index and draw following main conclusions:

- We confirm the steepening of the radio spectral index with increasing flux density [17–21]. The sources with higher flux are in general large in size and so the observed flux is largely radio emission from diffusion electrons, the diffusion spectral index is much steeper if compared with SNRs emission spectral index.
- The spectral index becomes independent of source size above ~ 50 arcsec. Assuming that the sources are roughly at redshift, $z = 1$, the 50 arcsec size corresponds to ~ 400 kpc (300 kpc, if at $z = 0.5$). The size independence of spectral index can be understood as the maximum possible radio emission from diffuse/convection electrons. Beyond this 50 arcsec size, the diffuse/convection electrons emit all their energy as radio and no escape is possible. We employ this saturated spectral index as a constraint on energy injection spectral index γ and SNRs

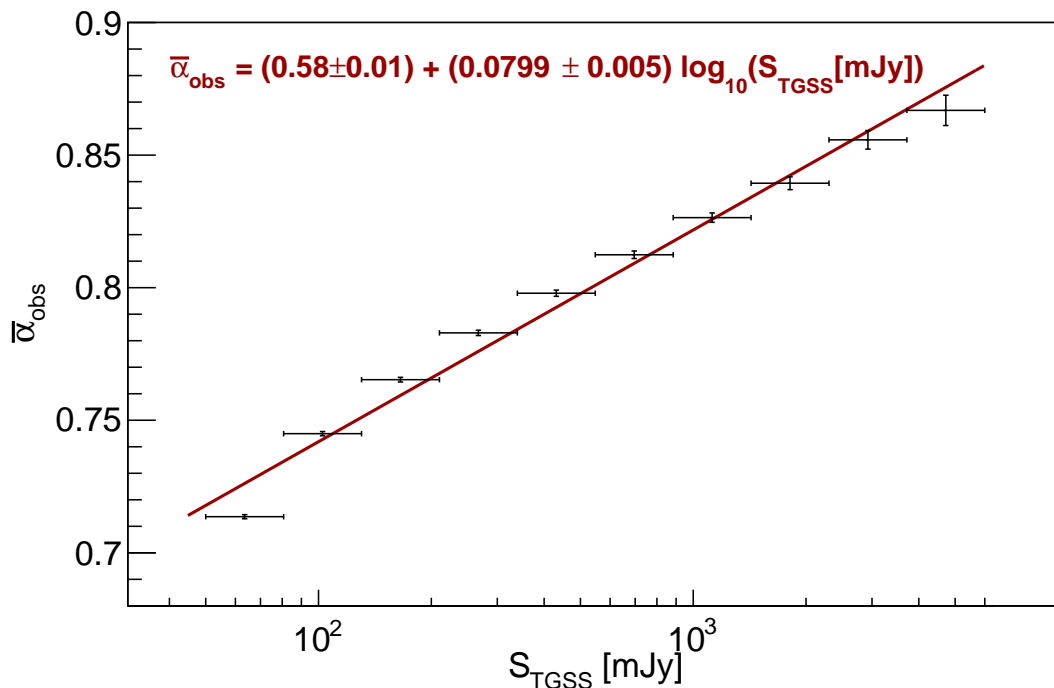


Figure 3: The mean radio spectral index, $\bar{\alpha}_{\text{obs}}$, as a function of flux density. The vertical error bars are the error in $\bar{\alpha}_{\text{obs}}$ in corresponding flux density bin.

contribution fraction. The result very much favours a low energy injection spectral index [22], $\gamma = 1.75 - 1.90$, and alternatively, a higher SNRs contribution $f_{\text{SNR}} = 10 - 25\%$ [6].

- We calculate the escape probability as a function of size for diffusion and convection propagation processes. For compact sources, the escape probability saturates to zero for reasonable values of γ and f_{SNR} ; in fact, it's saturation to zero indicates lower γ . The escape probability decreases very rapidly for convection propagation process. For diffusion processes, the escape probability is less steep. For very compact sources, the observed spectral index is close to ~ 0.4 , this indicate no diffusion contribution, the convection processes are likely to be dominating for these compact sources. The thermal emission may also be significantly contributing for these compact sources. As we only have integrated flux and the exact fraction of supernovae contribution is not known, more general conclusion can not be achieved.

7 Acknowledgments

This work is supported in part at the Technion by a fellowship from the Lady Davis Foundation and by the I-CORE Program of the Planning and Budgeting Committee, THE ISRAEL SCIENCE FOUNDATION (grants No. 1829/12 and No. 203/09), the Asher Space Research Institute. We thank Huib T. Intema (Leiden/NRAO) for answering queries related to TGSS catalog. We have used CERN ROOT 5.34/21 [24] for generating our plots.

References

- [1] P. Biermann, *On the radio continuum flux from the disks of spiral galaxies*, *A&A* **53** (Dec., 1976) 295–303.
- [2] J. J. Condon, *Radio emission from normal galaxies*, *ARAA* **30** (1992) 575–611.

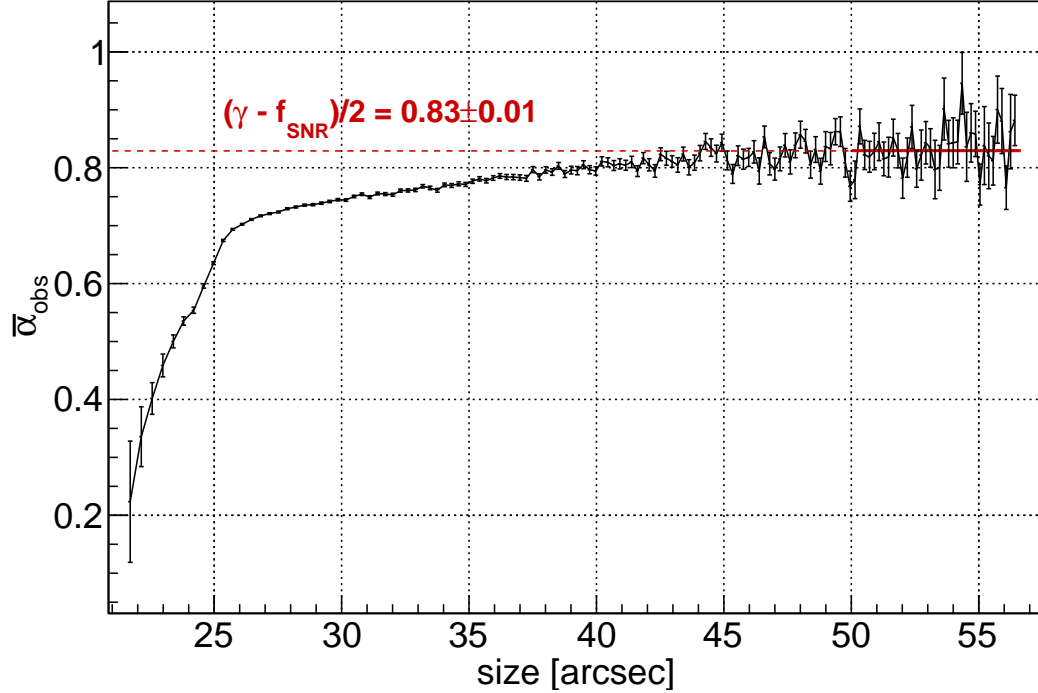


Figure 4: The mean radio spectral index, $\bar{\alpha}_{\text{obs}}$, dependence on size (\sqrt{ab}). The error bars represents the uncertainty in $\bar{\alpha}_{\text{obs}}$. The $\bar{\alpha}_{\text{obs}}$ dependence on size saturates very clearly for the sources above 50 arcsec (roughly 400 kpc, if assuming at redshift, $z \approx 1$). We find $\bar{\alpha}_{\text{obs}} = 0.83 \pm 0.01$ for these ultra large sources (fit above 50 arcsec).

- [3] D. A. Green, *VizieR Online Data Catalog: A Catalogue of Galactic Supernova Remnants (Green 1998)*, *VizieR Online Data Catalog* **7211** (Nov., 1998).
- [4] D. A. Green, S. P. Reynolds, K. J. Borkowski, U. Hwang, I. Harrus, and R. Petre, *The radio expansion and brightening of the very young supernova remnant G1.9+0.3*, *MNRAS* **387** (June, 2008) L54–L58, [[arXiv:0804.2317](#)].
- [5] G. Dubner and E. Giacani, *Radio emission from supernova remnants*, *A&A Rev.* **23** (Sept., 2015) 3, [[arXiv:1508.07294](#)].
- [6] U. Lisenfeld and H. J. Völk, *On the radio spectral index of galaxies*, *A&A* **354** (Feb., 2000) 423–430, [[astro-ph/9912232](#)].
- [7] H. T. Intema, P. Jagannathan, K. P. Mooley, and D. A. Frail, *The GMRT 150 MHz All-sky Radio Survey: First Alternative Data Release TGSS ADR1*, [[arXiv:1603.04368](#)].
- [8] J. J. Condon, W. D. Cotton, E. W. Greisen, Q. F. Yin, R. A. Perley, G. B. Taylor, and J. J. Broderick, *The NRAO VLA Sky Survey*, *AJ* **115** (May, 1998) 1693–1716.
- [9] A. Nusser and P. Tiwari, *The Clustering of Radio Galaxies: Biasing and Evolution Versus Stellar Mass*, *ApJ* **812** (2015), no. 1 85, [[arXiv:1505.06817](#)].
- [10] P. Tiwari and A. Nusser, *Revisiting the nvss number count dipole*, *Journal of Cosmology and Astroparticle Physics* **2016** (2016), no. 03 062, [[arXiv:1509.02532](#)].
- [11] G. Swarup, *Giant metrewave radio telescope (GMRT)*, in *IAU Colloq. 131: Radio Interferometry. Theory, Techniques, and Applications* (T. J. Cornwell and R. A. Perley, eds.), vol. 19 of *Astronomical Society of the Pacific Conference Series*, pp. 376–380, 1991.

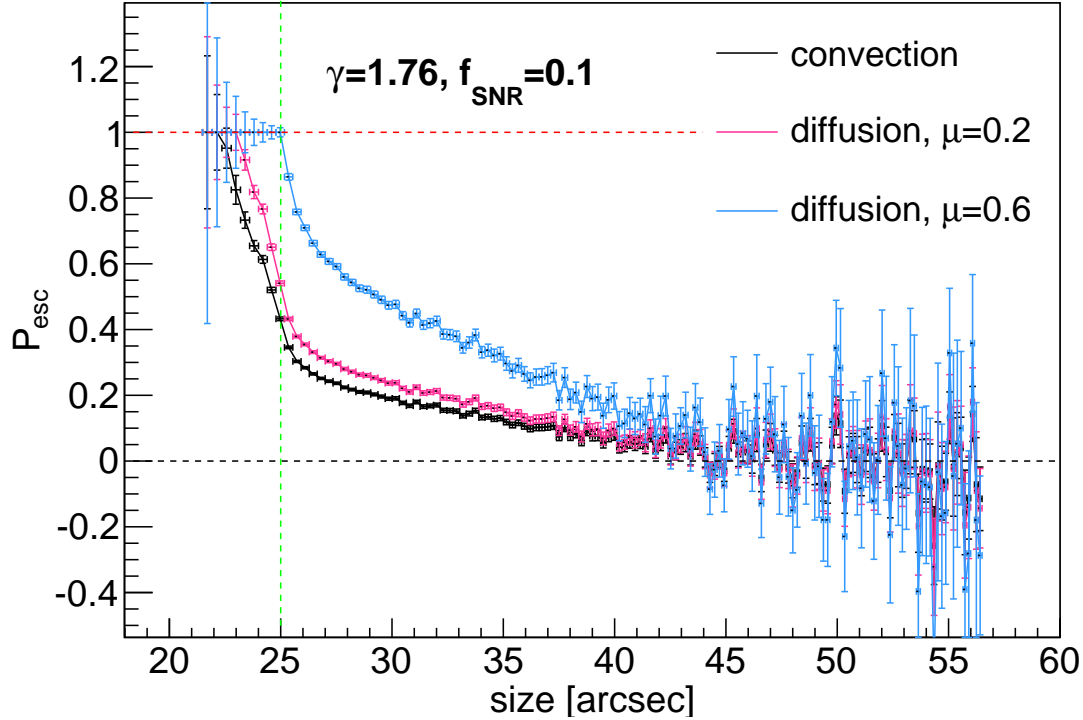


Figure 5: The escape probability with energy injection spectral index $\gamma = 1.76$ and 10% SNRs contribution in total flux. μ is the diffusion (diffusion coefficient $D(E) \propto E^\mu$) index. The vertical line, at $25''$, indicates the TGSS resolution limit. We have fixed $(\gamma - f_{\text{SNR}})/2 = 0.83$ to match the observed spectral index of large sources. For very compact sources, the mean radio spectral index $\bar{\alpha}_{\text{obs}}$ becomes equal or less than α_{SNR} and P_{esc} saturates at 1.

- [12] J. J. Condon and Q. F. Yin, *A new starburst model applied to the clumpy irregular galaxy Markarian 325*, *ApJ* **357** (July, 1990) 97–104.
- [13] M. S. Longair, *High energy astrophysics. Vol.1: Particles, photons and their detection*. Mar., 1992.
- [14] P. A. G. Scheuer, *Energetic particles in radio sources*, *Advances in Space Research* **4** (1984) 337–343.
- [15] M. Pohl and J. A. Esposito, *Electron Acceleration in Supernova Remnants and Diffuse Gamma Rays above 1 GeV*, *ApJ* **507** (Nov., 1998) 327–338, [[astro-ph/9806160](#)].
- [16] U. Lisenfeld, P. Alexander, G. G. Pooley, and T. Wilding, *Constraints on cosmic ray propagation from radio continuum data of NGC 2146.*, *MNRAS* **281** (July, 1996) 301–310, [[astro-ph/9603111](#)].
- [17] R. A. Windhorst, E. B. Fomalont, R. B. Partridge, and J. D. Lowenthal, *Microjansky source counts and spectral indices at 8.44 GHz*, *ApJ* **405** (Mar., 1993) 498–517.
- [18] I. Prandoni, P. Parma, M. H. Wieringa, H. R. de Ruiter, L. Gregorini, A. Mignano, G. Vettolani, and R. D. Ekers, *The ATESP 5 GHz radio survey. I. Source counts and spectral index properties of the faint radio population*, *A&A* **457** (Oct., 2006) 517–529, [[astro-ph/0607141](#)].
- [19] E. Ibar, R. J. Ivison, A. D. Biggs, D. V. Lal, P. N. Best, and D. A. Green, *Deep multi-frequency radio imaging in the Lockman Hole using the GMRT and VLA - I. The nature of the sub-mJy radio population*, *MNRAS* **397** (July, 2009) 281–298, [[arXiv:0903.3600](#)].
- [20] C. H. Ishwara-Chandra, S. K. Sirothia, Y. Wadadekar, S. Pal, and R. Windhorst, *Deep GMRT*

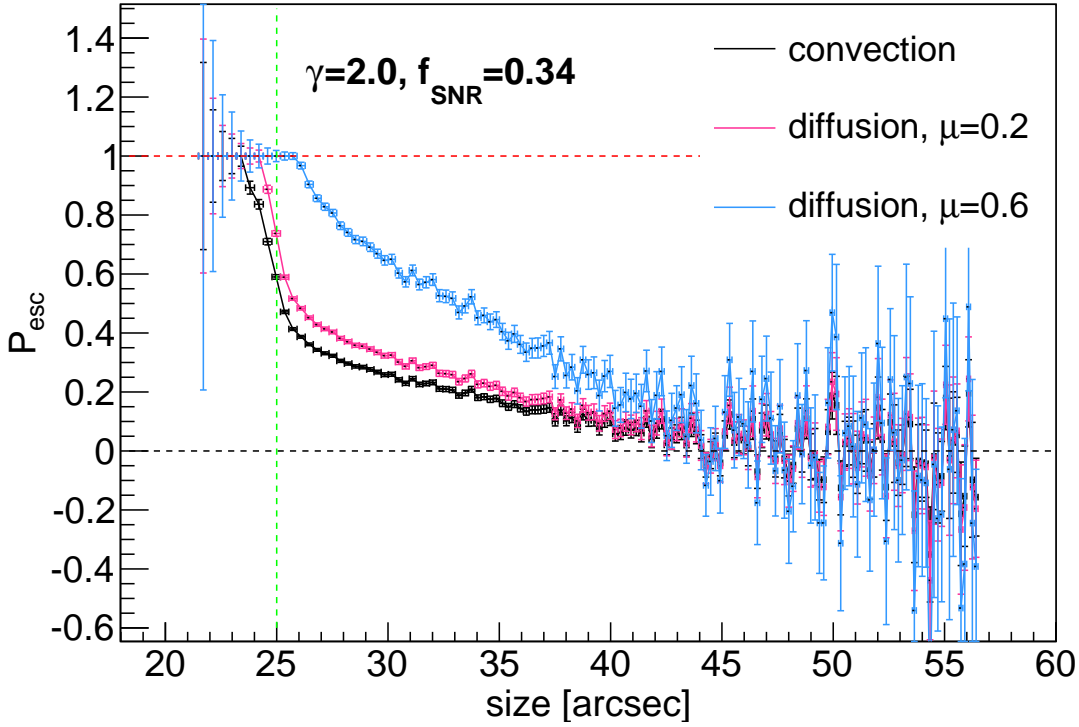
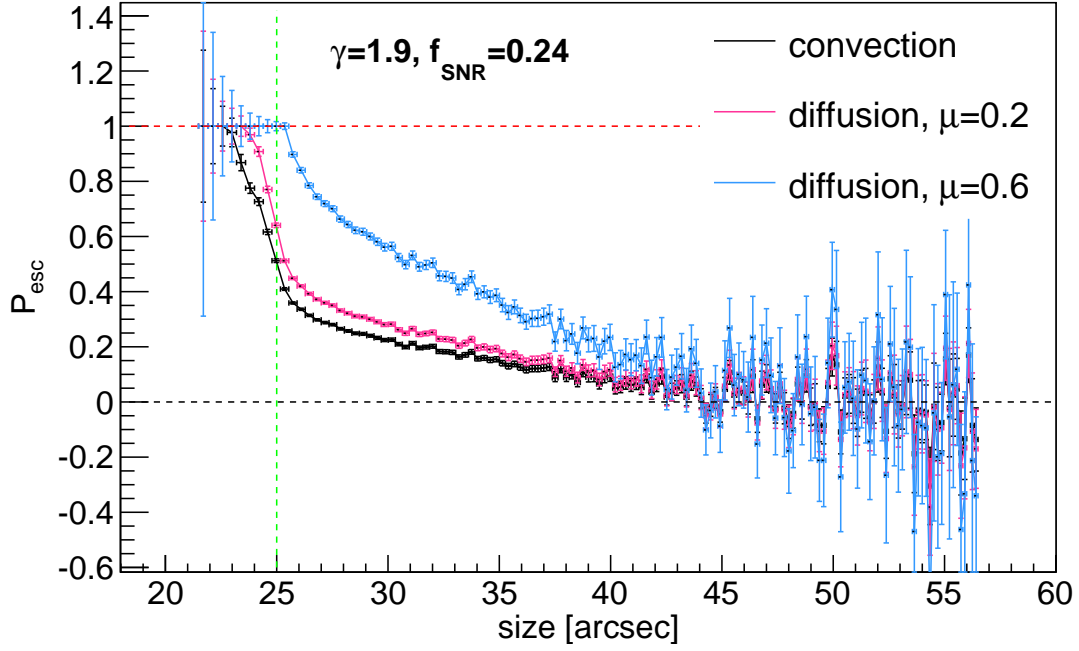


Figure 6: The escape probability with different energy injection spectral index γ and SNRs contribution. The very compact sources favour low γ value particularly if diffusion is the dominant cosmic ray propagation process.

150-MHz observations of the LBDS-Lynx region: ultrasteep spectrum radio sources, *MNRAS* **405** (June, 2010) 436–446, [[arXiv:1002.0691](#)].

- [21] K. E. Randall, A. M. Hopkins, R. P. Norris, P.-C. Zinn, E. Middelberg, M. Y. Mao, and R. G. Sharp, *Spectral index properties of milliJansky radio sources*, *MNRAS* **421** (Apr., 2012) 1644–1660, [[arXiv:1201.0568](#)].
- [22] E. G. Berezhko and H. J. Völk, *Kinetic theory of cosmic rays and gamma rays in supernova remnants. I. Uniform interstellar medium*, *Astroparticle Physics* **7** (Aug., 1997) 183–202.
- [23] M. Garcia-Munoz, J. A. Simpson, T. G. Guzik, J. P. Wefel, and S. H. Margolis, *Cosmic-ray propagation in the Galaxy and in the heliosphere - The path-length distribution at low energy*, *ApJ. S* **64** (May, 1987) 269–304.
- [24] R. Brun, F. Rademakers, et al., *ROOT web page*, <http://root.cern.ch/>, 2001.